

Closed-form Description of Microwave Signal Attenuation in Cellular Systems

Konstantinos B. BALTZIS

RadioCommunications Laboratory, Dept. of Physics, Aristotle University of Thessaloniki, Greece

kmpal@physics.auth.gr

Abstract. *The reliable and accurate description of signal attenuation characteristics is important in the simulation and performance analysis of wireless communications systems. Recent works have provided analytical expressions for the path loss statistics in cellular systems considering distance-dependent losses and shadowing. In this paper, we extend this analysis by including small-scale fading. A closed-form expression that gives the path loss density in a cellular network is given. The impact of channel parameters and cell size on signal attenuation is further investigated. Simulation results and comparisons with measured data in the literature verify the accuracy of the solution. The derived formulation is a useful tool for the modeling and analysis of cellular communications systems.*

Keywords

Microwave propagation, path loss, fading, composite gamma-lognormal density, cellular communications.

1. Introduction

The growth of wireless communications has spurred scientists toward the development of fast and reliable radio channel models. Nowadays, advanced propagation modeling that incorporates detailed representation of complicated propagation environments with sophisticated and computational efficient techniques are required to support new developments, [1-3].

An important issue in the study of wireless channels is the description of signal attenuation. Most of the developed models are based on empirical measurements over a given distance in a specific frequency range and a particular environment. For example, in [4], an ultra wideband (UWB) propagation model based on measurements taken at 5 GHz is presented. The model studies the UWB channel in the time and frequency domain and describes the median path loss and its random variation due to shadowing. In [5], path loss measurements at 60 GHz were used for the description of path loss and showed the correlation between propagation path length and channel attenuation. A narrowband elevation dependent shadowing model for mobile

systems that was based on measurements at the S and C bands was proposed in [6]. This model allowed the derivation of empirical formulas that assist in system-level simulation and availability estimation of wireless networks. However, a major drawback of empirical models is their dependence on system parameters and environmental characteristics that makes their accuracy in more general environments questionable. Complicated approaches have also been developed for the description of path loss (see, for example, [7]). There, a unified framework was introduced allowing the geometric characterization of fading. Proposals based on neural networks (NN) methods are also of great interest, [8]; they use measured or theoretical data and feed the NN input with the values of parameters such as the dimensions of buildings, roads, etc.

In the system-level simulations of wireless networks, path loss is usually estimated by positioning the nodes according to a known distribution and calculating the distances between them. Then, the application of a propagation model calculates the losses. In order to obtain correct results, the procedure is repeated many times; there is thus a trade-off between computational cost and solution accuracy. Therefore, the analytical description of path loss reduces the simulation time. Recently, the authors in [9] derived the probability density function (PDF) of the path loss between the center of a circular cell and a node distributed uniformly within this cell. An extension of this work in hexagonal areas is given in [10]. However, both models assume that nodes are moving with low velocity in a physically stationary environment and neglect small-scale (fast) fading.

In this paper, we extend [9] by comprising small-scale fading. This is usually modeled by the Nakagami- m distribution, [11-13]. Parameter m is the shape factor and it is related to the severity of fading. Shadowing (large-scale fading) is modeled by the lognormal distribution, [11-12]. In several cases, composite Nakagami-lognormal distribution models the combined effect of shadowing and small-scale fading, [11-12]. In this case, the local mean power is considered as a random variable; the instantaneous PDF of the signal-to-noise ratio is obtained by averaging the instantaneous Nakagami- m fading average power over the conditional pdf of lognormal shadowing.

The main contribution of this work is the closed-form description of the path loss density in a cellular network. In contrast to prior studies that consider distance-dependent losses and shadowing only, we further include small-scale fading. The impact of channel parameters and cell size on signal attenuation is investigated. Comparisons with simulation results and measured data in the literature verify the accuracy of the formulation. In our analysis, we assume that nodes are uniformly distributed within circular cells, assumptions that are common in the planning and simulation of cellular systems, [9], [14-15].

Rest of the paper is organized as follows: Section 2 discusses the modeling of fading channels. The proposed path loss PDF expression is given in Section 3. Results and discussions are provided in Section 4. Finally, Section 5 concludes the paper.

2. Lognormal and Nakagami- m Fading: General Principles

In the wireless environment, path loss increases exponentially with distance, [3], [16]. Usually, it is expressed in the log domain as:

$$L = L_0 + 10n \log(d/d_0) + X_S + Y, \quad d \geq d_0 \quad (1)$$

where L_0 (intercept value) is the path loss at a known reference distance d_0 , n is the path loss exponent, d is the distance between the transmitter and the receiver, X_S is the shadowing variation and Y is the small-scale fading term.

Shadowing is caused by large obstacles between the communicating nodes that attenuate signal power through absorption, reflection, scattering, and diffraction, [16]. It can be modeled as a lognormal random process; in this case, the PDF of the slowly varying signal power is

$$f_s(s) = \frac{\xi}{\sqrt{2\pi}\sigma_s} \exp\left(-\frac{(10 \log s - \mu)^2}{2\sigma^2}\right), \quad s > 0 \quad (2)$$

where μ and σ are the logarithmic mean and variance, respectively, and $\xi = 10/\ln 10 \approx 4.343$. Usually, e.g. [9], shadowing is modeled in the log-domain as a zero-mean Gaussian random variable with pdf

$$f_w(w) = \frac{1}{\sqrt{2\pi}\sigma} \exp\left(-\frac{w^2}{\sigma^2}\right). \quad (3)$$

Small-scale fading occurs over distances on the order of the signal wavelength when the channel coherence time is small relative to its delay constraints or the duration of the transmitted symbols, [16]. The Nakagami- m distribution is a good choice for its modeling; the PDF of the received signal power r is

$$f_r(r) = \frac{2}{\Gamma(m)} \left(\frac{m}{\Omega}\right)^m r^{2m-1} \exp\left(-\frac{mr^2}{\Omega}\right), \quad m \geq 0.5 \quad (4)$$

where $\Gamma(\cdot)$ is the gamma function and Ω denotes the local mean received power. The distribution includes the Rayleigh and the one-side of the Gaussian distribution for $m=1$ and $m=0.5$, respectively. There is also a simple one-to-one mapping between m and Rician k factor that allows Nakagami- m to approximate the Rician distribution, [12]. In the limit $m \rightarrow \inf$, (4) tends to a Dirac's function and describes the absence of small-scale fading.

3. Path Loss Density Expression

In this Section, the path loss density given in [9] is extended and comprises small-scale fading. Recall that the combined effect of shadowing and small-scale fading can be modeled by the composite Nakagami-lognormal distribution. In this case, the received signal power follows a gamma-lognormal distribution with pdf given, [11], by

$$f_c(x) = \int_0^{+\infty} \left\{ \frac{\xi m^m x^{m-1}}{\sqrt{2\pi}\Gamma(m)\sigma z^{m+1}} \times \exp\left(-\frac{mx}{z} - \frac{(10 \log \Omega - \mu)^2}{2\sigma^2}\right) \right\} dz \quad (5)$$

To the best of the author's knowledge, $f_c(x)$ cannot be given in closed form; however, we can accurately approximate it by a lognormal distribution with logarithmic mean and variance

$$\mu_c = \mu + \xi[\Psi(m) - \ln m], \quad (6)$$

$$\sigma_c^2 = \sigma^2 + \xi^2 \zeta(2, m) \quad (7)$$

where $\Psi(\cdot)$ and $\zeta(\cdot; \cdot)$ are the Euler's psi and Hurwitz zeta functions, respectively.

Taking into consideration (2) and (3) and setting

$$\mu_{c,0} = \xi[\Psi(m) - \ln m] \quad (8)$$

we obtain from (5)-(7) that the combined fading density in the log-domain can be expressed as

$$f_w'(w) = \frac{1}{\sqrt{2\pi}\sigma_c} \exp\left(-\frac{(w - \mu_{c,0})^2}{2\sigma_c^2}\right). \quad (9)$$

Under the assumption of uniform node distribution, the PDF of the distance of a node at a distance x from the center of a circular cell with radius R is

$$f_x(x) = \begin{cases} 2x/R^2, & 0 \leq x \leq R \\ 0, & x \geq R \end{cases} \quad (10)$$

Then, the PDF of the random variable $y = 10n \log x$ is

$$f_y(y) = \frac{2}{n\xi R^2} \exp\left(\frac{2y}{n\xi}\right), \quad y < 10n \log R. \quad (11)$$

The PDF of the sum of two independent random variables is the convolution of their PDFs. Because

$$\int \exp(-px^2 + qx) dx = \sqrt{\frac{\pi}{4p}} \exp\left(\frac{q^2}{4p}\right) \times \operatorname{erf}\left(\frac{2px - q}{2\sqrt{p}}\right) \quad (12)$$

we obtain, after some manipulation, that the density of the sum of distance-dependent loss and combined fading is

$$f_z(z) = \int_{-\infty}^{\infty} f_w'(w) f_Y(z-w) dw = \frac{1}{n\xi R^2} \exp\left(2\left[\frac{z - \mu_{c,0}}{n\xi} + \left(\frac{\sigma_c}{n\xi}\right)^2\right]\right) \times \operatorname{erfc}\left(\frac{z - 10n \log R - \mu_{c,0} + \sqrt{2}\sigma_c}{\sqrt{2}\sigma_c} + \frac{\sqrt{2}\sigma_c}{n\xi}\right) \quad (13)$$

The sum of a random variable and a constant is a new random variable with PDF equal to the shifted PDF of the initial one. As a result, (1) and (13) give that the path loss PDF is

$$f_L(l) = \frac{1}{n\xi R^2} \exp\left(2\left[\frac{l - L_0 - \mu_{c,0}}{n\xi} + \left(\frac{\sigma_c}{n\xi}\right)^2\right]\right) \times \operatorname{erfc}\left(\frac{l - L_0 - 10n \log R - \mu_{c,0} + \sqrt{2}\sigma_c}{\sqrt{2}\sigma_c} + \frac{\sqrt{2}\sigma_c}{n\xi}\right) \quad (14)$$

A similar expression that neglected small-scale fading was derived in [9]. In that case, the path loss PDF was

$$f_L^0(l) = \frac{1}{n\xi R^2} \exp\left(2\left[\frac{l - L_0}{n\xi} + \left(\frac{\sigma}{n\xi}\right)^2\right]\right) \times \operatorname{erfc}\left(\frac{l - L_0 - 10n \log R + \sqrt{2}\sigma}{\sqrt{2}\sigma} + \frac{\sqrt{2}\sigma}{n\xi}\right) \quad (15)$$

Notice that replacing σ with σ_c and L_0 with

$$L_{0,c} = L_0 + \mu_{c,0} \quad (16)$$

into (15), we obtain (14). It easily comes from (7) and (8) that the two PDFs coincide at great values of m .

4. Results and Discussion

In this Section, representative examples explore the relation between environmental parameters and path loss density. The analysis focuses on the study of the impact of small-scale fading on the PDF curves. Comparisons with simulation and measured results verify the accuracy of our proposal. In the cases we study, mobile nodes are uniformly distributed within a circular cell and the base station is located at the center of cell.

In order to verify the accuracy of (14), we present in Fig. 1 simulation and numerical results for $m = 1$ (Rayleigh fading) and $m = 3$ (typical value in wireless systems, [17]). In the simulations, shadowing and small-scale fading were modeled as lognormal and Nakagami- m random variables,

respectively. We set $n = 3.4$, $\sigma = 6$ dB and $L_0 = 37$ dB (typical UMTS air interface parameters), [18]. Cell radius was 100 m. In each snapshot, a single node was generated and randomly positioned within the cell, see (10). Then, the distance-dependent, shadowing and small-scale fading losses were calculated. After one path loss estimation, another snapshot continued. For each curve, 10^5 independent runs were performed. The simulation values in Fig. 1 were averaged over a path loss step-size of 1 dB. Good agreement between the theoretical values and the simulation results is observed. We notice that decrease in m flattens the pdf curve and shifts it slightly to the left.

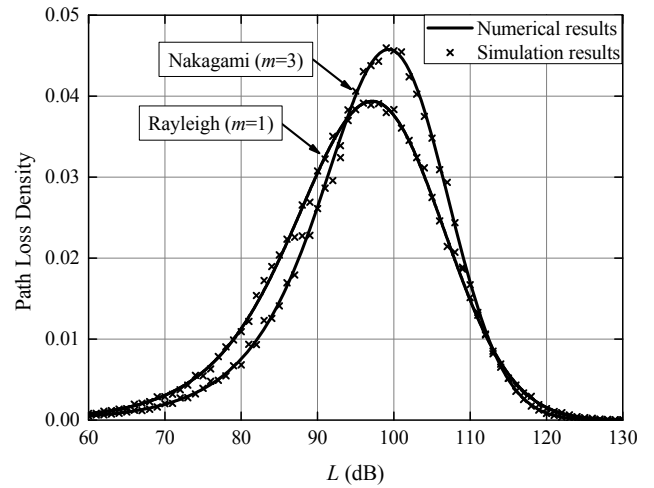


Fig. 1. Path loss density: Numerical and simulation results.

The proposed formulation is further validated through comparisons with measured data. The authors in [19] presented the results of broadband channel measurements at 5.2 GHz in an urban macro-cell environment. The receiver was located above rooftop at a high building and the transmitter was mounted at street level and moved at 21 km/h; the difference in height between transmitting and receiving antenna was 52 m. Under such conditions, a path loss exponent $n = 3.5$ is expected, [20]. Measurement area was divided into three regions: the first was a circle with radius 180 m; the other two regions where the concentric annuluses defined between 180 m and 400 m and from 400 m to 800 m. The received signals consisted of both line- and non line-of-sight components. The measured data were processed in the time domain for different points in time after the removal of thermal noise effects. The results (Table I, SG1 scenario, 1st row, [19]) are given in Tab. 1. In the same table, the corresponding numerical values based on (14) are given for various m . To the best of the author's knowledge, there is no campaign measurement to provide us with empirical data for the shape factor in this scenario. However, values of m reported in literature can approximately be used in our study. A value that approaches mostly the specific measurement conditions was derived in [13]. There, a measurement campaign for the estimation of the range of m was preformed in an urban area at 900 MHz. In these measurements, the difference in heights between transmitter and receiver was 35 m and the

receiver was moving at a constant speed of 20 km/h. It was found that m ranged from 0.5 to 3.5 and its average was 1.56. The values $m = 2$ and $m = 3$ are common in the modeling and analysis of wireless systems, [17], [21]. In order to compare our results with [9], results based on (15) are also presented. Calculations were made for $L_0 = 37$ dB and $\sigma = 6$ dB, as in the previous example. Numerical results are very close to the measured values (esp. when $m = 2$). However, notice that m does not affect significantly the calculated average path loss.

$R(m)$	Meas. ^[a]	Numerical results ^[b]			
		$m = 1.56$	$m = 2$	$m = 3$	$m \rightarrow \text{inf}$ [9]
180	107.3	106.8	107.2	107.6	108.3
400	119.4	118.9	119.3	119.7	120.5
800	129.2	129.5	129.8	130.2	131

Tab. 1. Measured, [a], and calculated, [b], average path loss (in dB).

Next, representative results demonstrate the impact of channel parameters on path loss PDF curves. Fig. 2 shows $f_L(l)$ for some sample values of m . The rest of the system parameters are $n = 3.4$, $\sigma = 6$ dB, $L_0 = 37$ dB and $R = 100$ m. The PDF curves flatten and shift to the left as m decreases. In this case, the impact of the variation of shape factor on the PDF curves increases.

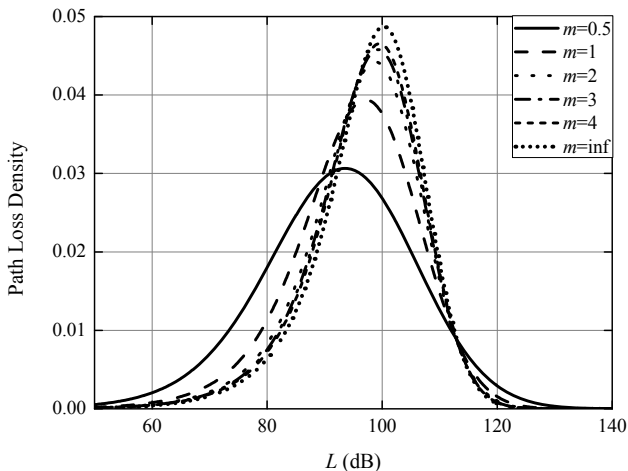


Fig. 2. Impact of the shape factor on the path loss density.

The impact of shadowing and distance-dependent loss, on the PDF curve is illustrated for varied shape factor in Figs. 3 and 4, respectively. In outdoor communications, σ and n usually range between 4 and 10 dB and from 2 to 6, correspondingly, [22]. The rest of the system parameters are left unchanged. Fig. 3 shows that increase in σ slightly flattens and shifts PDF curves to the left (the severity of shadowing increases with σ). Moreover, the impact of the variation of σ increases with m , i.e. as the amount of small-scale fading decreases. Similarly, as σ decreases the impact of the variation of m is more significant. As n increases, PDF curves flatten, their shapes change rapidly and they shift to the right due to the increased distance-dependent path loss, see Fig. 4. Also notice that the lower the n , the greater the impact of the variation of m .

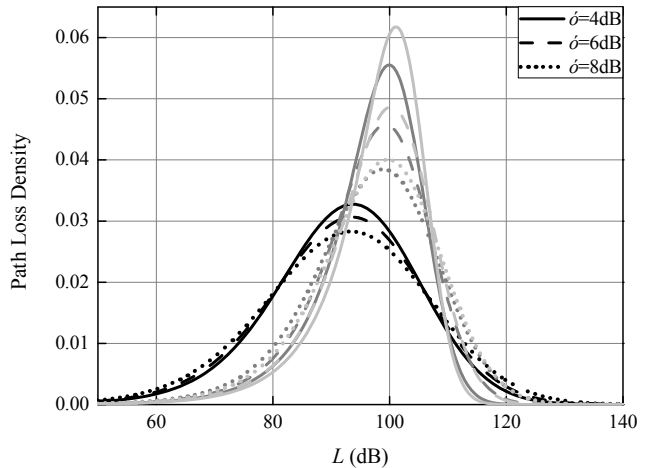


Fig. 3. Impact of shadowing on $f_L(l)$ for $m=0.5$ (black curves), $m=3$ (gray curves) and $m \rightarrow \text{inf}$ (light gray curves).

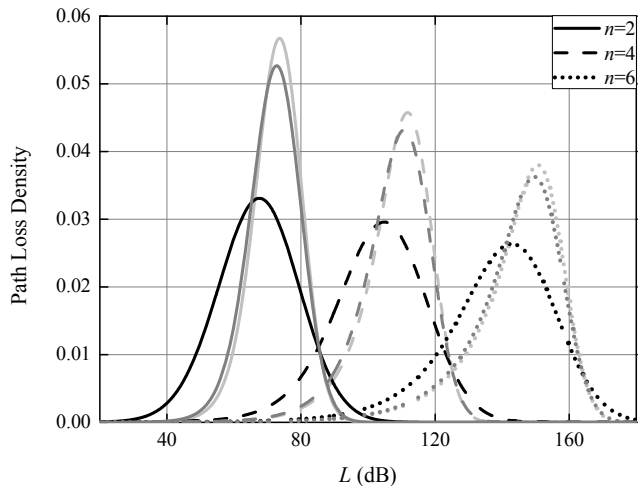


Fig. 4. Impact of n on path loss PDF for $m=0.5$ (black curves), $m=3$ (gray curves) and $m \rightarrow \text{inf}$ (light gray curves).

Finally, Figs. 5 and 6 show that as L_0 or R vary (the rest of the system parameters are as before) $f_L(l)$ shifts along the l -axis. This shift does not depend on m .

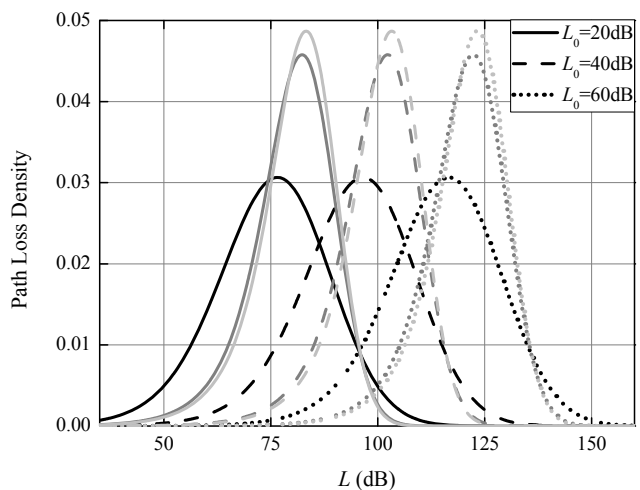


Fig. 5. Impact of L_0 on $f_L(l)$ for $m=0.5$ (black curves), $m=3$ (gray curves) and $m \rightarrow \text{inf}$ (light gray curves).

Fig. 5 shows that change in the intercept value shifts equally the pdf curve along the l -axis. Moreover, the shift of the curves decreases with cell size, see Fig. 6 (the author believes that the extended analysis of the last issue is beyond the scope of this paper; for further information, see [10]).

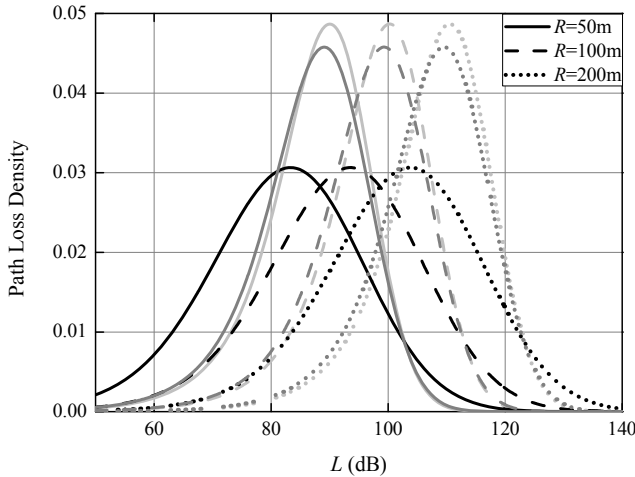


Fig. 6. Impact of cell radius on $f_L(l)$ for $m=0.5$ (black curves), $m=3$ (gray curves) and $m \rightarrow \infty$ (light gray curves).

It was shown that (15) can describe small-scale fading by replacing σ and L_0 with σ_c and $L_{0,c}$, respectively. At this point, we propose as a measure of the contribution of small-scale fading on combined fading the quantities

$$\begin{aligned} S &\equiv \sigma_c^2 / \sigma^2 \\ \Lambda &\equiv L_{0,c} / L_0 \end{aligned} \quad (1)$$

As the two ratios approach unity, the contribution of small-scale fading diminishes. In Figs. 7 and 8, the dependence of S and Λ on channel parameters is explored. Fig. 7 shows that as shadowing decreases, small-fading becomes more significant. Moreover, small-scale fading is always important at small values of m . In Fig. 8, we observe that the dependence of Λ on m is significant at low m . Notice also that the impact of m on Λ decreases with L_0 .

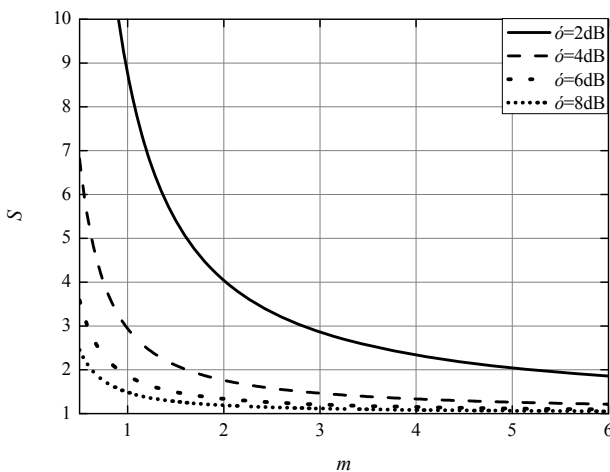


Fig. 7. Impact of m and σ on parameter S .

Small-scale fading affects system performance significantly, especially when shadowing and/or distance-dependent loss are small. Moreover, it modifies the impact of the rest of the channel parameters on signal attenuation statistics. Our analysis has shown that small-scale fading should always be considered in the study of a cellular network when shape factor, shadowing deviation, path loss exponent and intercept value are small.

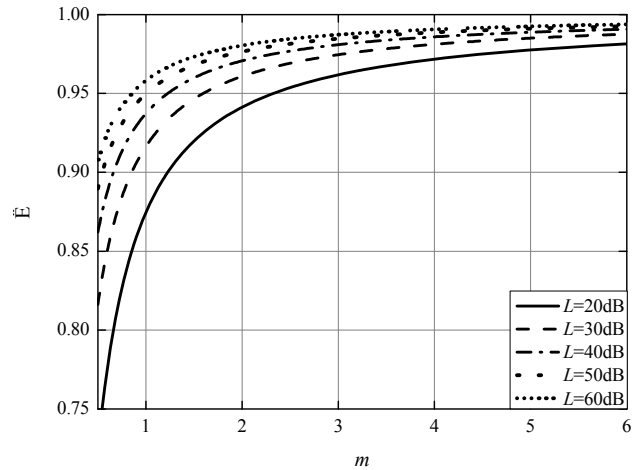


Fig. 8. Impact of m and σ on parameter Λ .

5. Conclusions

In this paper, we derived a closed-form expression for the path loss density in cellular networks. Its main contribution is the consideration of small-scale fading. The impact of channel parameters and cell size on path loss was investigated and provided with interesting results. The paper also discusses the importance of the consideration of small-scale fading on system analysis. Not only it degrades system performance, but also modifies the way in which the rest of the channel parameters affect path loss density. Use of the proposed formulation assists in network planning and design and reduces computational complexity; compared to other proposals, it is more suitable for the simulation and analysis of cellular networks when small-scale fading is comparable to the rest of the signal attenuation factors.

References

- [1] WIESER, V., PSENAK, V. Performance of advanced hybrid link adaptation algorithms in mobile radio channel. *Radioengineering*, 2008, vol. 17, no. 3, p. 81-86.
- [2] NOORI, N., KARIMZADEH-BAEE, R., ABOLGHASEMI, A. An empirical ultra wideband channel model for indoor laboratory environments. *Radioengineering*, 2009, vol. 18, no. 1, p. 68-74.
- [3] BALTZIS, K. B. Current issues and trends in wireless channel modeling and simulation. *Recent Patents on Computer Science*, 2009, vol. 2, no. 3, p. 166-177.

- [4] GHASSEMZADEH, S. S., JANA, R., RICE, C. W., TURIN, W., TAROKH, V. Measurement and modeling of an ultra-wide bandwidth indoor channel. *IEEE Transactions on Communications*, 2004, vol. 52, no. 10, p. 1786-1796.
- [5] MORAITIS, N., CONSTANTINOU, P. Indoor channel measurements and characterization at 60 GHz for wireless local area network applications. *IEEE Transactions on Antennas and Propagation*, 2004, vol. 52, no. 12, p. 3180-3189.
- [6] HOLIS, J., PECHAC, P. Elevation dependent shadowing model for mobile communications via high altitude platforms in built-up areas. *IEEE Transactions on Antennas and Propagation*, 2008, vol. 56, no. 4, p. 1078-1084.
- [7] HAENGGI, M. A geometric interpretation of fading in wireless networks: Theory and applications. *IEEE Transactions on Information Theory*, 2008, vol. 54, no. 12, p. 5500-5510.
- [8] CERRI, G., CINALLI, M., MICHETTI, F., RUSSO, P. Feed forward neural networks for path loss prediction in urban environment. *IEEE Transactions on Antennas and Propagation*, 2004, vol. 52, no. 11, p. 3137-3139.
- [9] BHARUCHA, Z., HAAS, H. The distribution of path losses for uniformly distributed nodes in a circle. *Research Letters in Communications*, 2008, vol. 2008, article ID 376895, 4 pages. DOI: 10.1155/2008/376895.
- [10] BALTZIS, K. B. Analytical and closed-form expressions for the distribution of path loss in hexagonal cellular networks. *Wireless Personal Communications*, submitted for publication.
- [11] ALOUINI, M.-S., GOLDSMITH, A. J. Area spectral efficiency of cellular mobile radio systems. *IEEE Transactions on Vehicular Technology*, 1999, vol. 48, no. 4, p. 1047-1066.
- [12] SIMON, M. K., ALOUINI, M.-S. *Digital Communication over Fading Channels*. 2nd ed. Chichester: John Wiley & Sons, Ltd, 2005.
- [13] RUBIO, L., REIG, J., CARDONA, N. Evaluation of Nakagami fading behaviour based on measurements in urban scenarios. *AEU - International Journal of Electronics and Communications*, 2007, vol. 61, no. 2, p. 135-138.
- [14] XIAO, L., GREENSTEIN, L., MANDAYAM, N., PERIYALWAR, S. Distributed measurements for estimating and updating cellular system performance. *IEEE Transactions on Communications*, 2008, vol. 56, no. 6, p. 991-998.
- [15] BALTZIS, K. B., SAHALOS, J. N. A low-complexity 3-D geometric model for the description of CCI in cellular systems. *Electrical Engineering*, 2009, vol. 91, no. 4, p. 211-219.
- [16] PARSONS, J. D. *The Mobile Radio Propagation Channel*. Chichester: John Wiley & Sons, Ltd, 2000.
- [17] KILLAT, M., HARTENSTEIN, H. An empirical model for probability of packet reception in vehicular ad hoc networks. *EURASIP Journal on Wireless Communications and Networking*, 2009, vol. 2009, article ID 721301, 12 pages. DOI: 10.1155/2009/721301.
- [18] OMIYI, P., HAAS, H., AUER, G. Analysis of TDD cellular interference mitigation using busy-bursts. *IEEE Transactions on Wireless Communications*, 2007, vol. 6, no. 7, p. 2721-2731.
- [19] THIELE, L., JUNGNICKEL, V. Out-of-channel statistics at 5.2 GHz. In *Proceedings of the First European Conference on Antennas and Propagation (EuCAP 2006)*, Nice (France), 2006, p. 1-6. DOI: 10.1109/EUCAP.2006.4584756.
- [20] ZHAO, X., KIVINEN, J., VAINIKAINEN, P., SKOG, K. Propagation characteristics for wideband outdoor mobile communications at 5.3 GHz. *IEEE Journal on Selected Areas in Communications*, 2002, vol. 20, no. 3, p. 507-514.
- [21] CHAN, N. H. L., MATHIOPOULOS, P. T. Efficient video transmission over correlated Nakagami fading channels for IS-95 CDMA systems. *IEEE Journal on Selected Areas in Communications*, 2000, vol. 18, no. 6, p. 996-1011.
- [22] RAPPAPORT, T. S. *Wireless Communications: Principles and Practice*. 2nd ed. Upper Saddle River: Prentice Hall PTR, 2002.

About Author...

Konstantinos B. BALTZIS was born in Thessaloniki, Greece. He received his B.Sc. degree in Physics in 1996, his M.Sc. degree in Electronics and Communications in 1999 and his PhD degree in Communications Engineering in 2005, all from the Aristotle University of Thessaloniki (AUTH), Greece. He is a member of the permanent research staff of the RadioCommunications Laboratory of AUTH and works as a part-time assistant professor in the Department of Automation at the Alexander Technological Educational Institute of Thessaloniki. He is also a teaching staff member in the Program of Postgraduate Studies in Electronic Physics of AUTH. His current research interests include wireless networks, propagation, antennas, microwave systems and evolutionary optimization methods.